

Responses to comments by editor and reviewer #2

Comments by editor

Both referees have evaluated your revised manuscript. The referee #1 provided several suggestions for a further minor revision. Please see the report. Regarding the comment on Figure 4, I suggest defining the abbreviations "AN_" and "BB_" in the figure caption, as the regions have been named in Figure 1.

Response: We appreciate the suggestion. The abbreviations are defined as suggested, i. e., Lines 772-773 "Figure 4. Contributions of anthropogenic sources (prefixed "AN_" in the legend) and open biomass burning ("BB_"...)".

Comments by reviewer #2

The authors well solved my concerns in the revised manuscript. I only have few minor comments now. Please see below:

Line 92: The observed BC concentration could be biased by a factor of 2 in Sharma et al. (2017).

Response: In light of the point, the sentence is revised to reflect the larger bias of 2 in Lines 92-93 to "The observations of BC that are used for model comparisons may be biased by a factor of 2 depending on the method used (Sinha et al., 2017; Sharma et al., 2017)".

Line 132: Please define 5000 m as "high altitudes" here.

Response: Revised in Line 133-134 from "...5000 m (4750–5250 m), were simulated" to "... high altitudes (4750–5250 m), were simulated". Relevant corrections were done through the context to avoid iteration.

Figure 4: Please present the full name before using the abbreviations (e.g., AN_EUR).

Response: The abbreviations are added in the figure caption in Lines 772-773 as "Figure 4. Contributions of anthropogenic sources (prefixed "AN_" in the legend) and open biomass burning ("BB_"...)".

Line 48: Many recent studies examined the impact of BC on Arctic climate (e.g., Sand et al., 2016; Yang et al., 2019). In addition to BC, tropospheric ozone, methane, other short-lived climate forcers, like sulfate aerosol (Yang et al., 2018), could also affect the Arctic climate.

Response: These recent progresses were added in L48-49 as "Short-lived climate pollutants such as black carbon (BC) particles (e.g., Sand et al., 2016; Yang et al., 2019), sulfate aerosol (Yang et al., 2018), tropospheric ozone, ...", and corresponding references added.

Technical correction:

Line 140, "life time" is corrected to "lifetime".

1 **Flexpart v10.1 simulation of source contributions to Arctic black carbon**

2

3 Chunmao Zhu¹, Yugo Kanaya^{1,2}, Masayuki Takigawa^{1,2}, Kohei Ikeda³, Hiroshi Tanimoto³,

4 Fumikazu Taketani^{1,2}, Takuma Miyakawa^{1,2}, Hideki Kobayashi^{1,2}, Ignacio Pissó⁴

5

6 ¹Research Institute for Global Change, Japan Agency for Marine–Earth Science and
7 Technology (JAMSTEC), Yokohama 2360001, Japan

8 ²Institute of Arctic Climate and Environmental Research, Japan Agency for Marine–Earth
9 Science and Technology, Yokohama 2360001, Japan

10 ³National Institute for Environmental Studies, Tsukuba 305-8506, Japan

11 ⁴NILU – Norwegian Institute for Air Research, Kjeller 2027, Norway

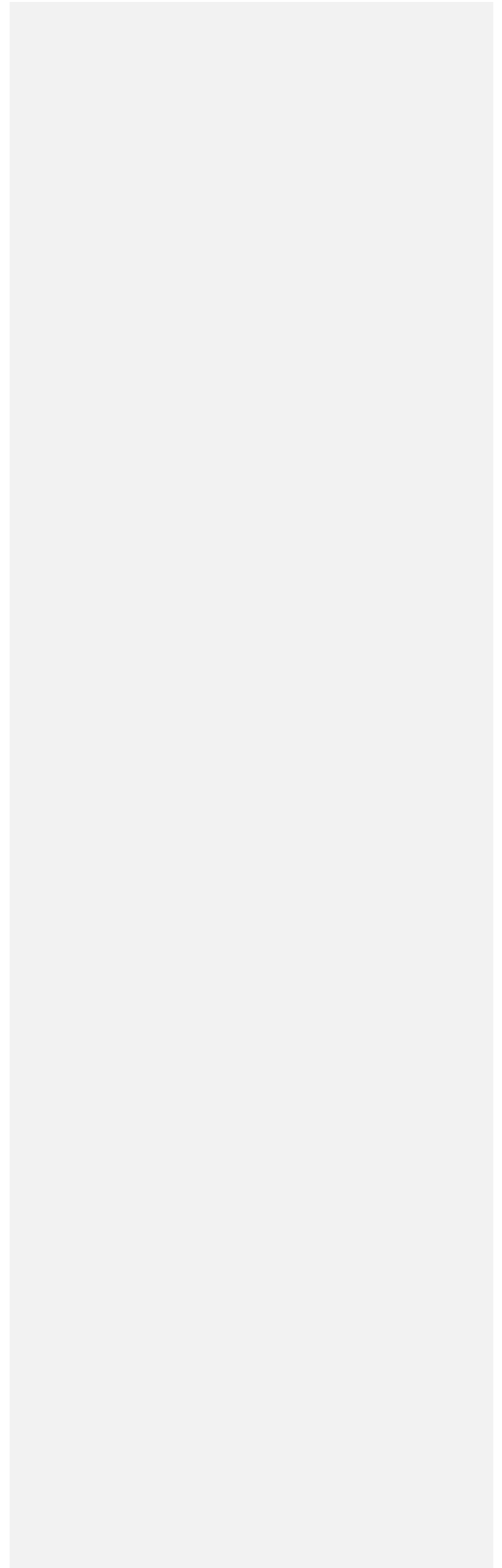
12

13 Correspondence to Chunmao Zhu (chmzhu@jamstec.go.jp)

14 **Abstract**

15 The Arctic environment is undergoing rapid changes such as faster warming than the
16 global average and exceptional melting of glaciers in Greenland. Black carbon (BC) particles,
17 which are a short-lived climate pollutant, are one cause of Arctic warming and glacier
18 melting. However, the sources of BC particles are still uncertain. We simulated the potential
19 emission sensitivity of atmospheric BC present over the Arctic (north of 66° N) using the
20 Flexpart Lagrangian transport model (version 10.1). This version includes a new aerosol wet
21 removal scheme, which better represents particle-scavenging processes than older versions
22 did. Arctic BC at the surface (0–500 m) and high altitudes (4750–5250 m) is sensitive to
23 emissions in high latitude (north of 60° N) and mid-latitude (30–60° N) regions, respectively.
24 Geospatial sources of Arctic BC were quantified, with a focus on emissions from
25 anthropogenic activities (including domestic biofuel burning) and open biomass burning
26 (including agricultural burning in the open field) in 2010. We found that anthropogenic
27 sources contributed 82 % and 83 % of annual Arctic BC at the surface and high altitudes,
28 respectively. Arctic surface BC comes predominantly from anthropogenic emissions in
29 Russia (56 %), with gas flaring from the Yamalo-Nenets Autonomous Okrug and Komi
30 Republic being the main source (31 % of Arctic surface BC). These results highlight the need
31 for regulations to control BC emissions from gas flaring to mitigate the rapid changes in the
32 Arctic environment. In summer, combined open biomass burning in Siberia, Alaska, and
33 Canada contributes 56–85 % (75 % on average) and 40–72 % (57 %) of Arctic BC at the
34 surface and high altitudes, respectively. A large fraction (40 %) of BC in the Arctic at high
35 altitudes comes from anthropogenic emissions in East Asia, which suggests that the rapidly
36 growing economies of developing countries could have a non-negligible effect on the Arctic.
37 To our knowledge, this is the first year-round evaluation of Arctic BC sources that has been

38 performed using the new wet deposition scheme in Flexpart. The study provides a scientific
39 basis for actions to mitigate the rapidly changing Arctic environment.
40



41 1 Introduction

42 The Arctic region has experienced warming at a rate twice that of the global average in
43 recent decades (Cohen et al., 2014). The Arctic cryosphere has been undergoing
44 unprecedented changes since the mid-1800s (Trusel et al., 2018). Glacier cover in Greenland
45 reached its historically lowest level in summer 2012 (Tilling et al., 2015). Evidence indicates
46 that the emissions and transport of greenhouse gases and aerosols to the Arctic region are
47 contributing to such warming and melting of snow and ice (Keegan et al., 2014; Najafi et al.,
48 2015). Short-lived climate pollutants such as black carbon (BC) particles ([e.g., Sand et al.,
49 2016; Yang et al., 2019](#)), [sulfate aerosol \(Yang et al., 2018\)](#), tropospheric ozone, and
50 methane greatly affect the Arctic climate (AMAP, 2015; Quinn et al., 2008).

51 BC particles are emitted during incomplete combustion of fossil fuels, biofuels, and
52 biomass. BC warms the atmosphere by direct absorption of solar radiation. The deposition
53 of BC on snow and ice surfaces accelerates their melting through decreasing albedo, which
54 contributes to the rapid loss of glaciers. In the Arctic region, ground-based observations
55 have indicated that BC shows clear seasonal variations, with elevated mass concentrations
56 in winter and spring (the so-called Arctic haze) and low values in summer (Law and Stohl,
57 2007). Such seasonal variations are explained by increased transport from lower latitudes in
58 the cold season and increased wet scavenging in the warm season (Shaw, 1995; Garrett et
59 al., 2011; Shen et al., 2017).

60 The presence of BC particles in the Arctic is mainly attributed to emissions in high-latitude
61 regions outside the Arctic, such as northern Europe and Russia (Stohl, 2006; Brock et al.,
62 2011). This is partly caused by the polar dome (Stohl, 2006), which is formed because of the
63 presence of constant potential temperature near the surface. The emissions in high-latitude
64 regions are transported to the Arctic region and trapped in the dome, which increases the

65 surface concentration. Recently, Schmale et al. (2018) suggested that local emissions from
66 within the Arctic are another important source, and these are expected to increase in the
67 future.

68 Although numerous studies have been performed, results regarding regional
69 contributions of BC sources in the Arctic are still inconclusive. For example, ground-based
70 observations and Lagrangian transport model results reported by Winiger et al. (2016)
71 showed that BC in Arctic Scandinavia is predominantly linked to emissions in Europe. Over
72 the whole Arctic region (north of 66° N), Russia contributes 62 % to surface BC in terms of
73 the annual mean (Ikeda et al., 2017). Gas flaring in Russia has been identified as a major
74 (42 %) source of BC at the Arctic surface (Stohl et al., 2013). Xu et al. (2017) found that
75 anthropogenic emissions from northern Asia contribute 40–45 % of Arctic surface BC in
76 winter and spring. However, the results of some other studies have suggested that Russia,
77 Europe, and South Asia each contribute 20–25 % of BC to the low-altitude springtime Arctic
78 haze (Koch and Hansen, 2005). Sand et al. (2016) found that the surface temperature in the
79 Arctic is most sensitive to emissions in Arctic countries, and Asian countries contribute
80 greatly to Arctic warming because of the large absolute amount of emissions. With these
81 large disagreements among studies, it is thus necessary to unveil BC sources in the Arctic
82 with high precision simulations.

83 Various models have been used to investigate BC sources in the Arctic. Depending on the
84 simulation method, these models are generally categorized as Lagrangian transport models
85 (Hirdman et al., 2010; Liu et al., 2015; Stohl et al., 2006, 2013), chemical transport models
86 (Ikeda et al., 2017; Koch and Hansen, 2005; Qi et al., 2017; Shindell et al., 2008; Wang et al.,
87 2011; Xu et al., 2017), and global climate models (Ma et al., 2013; Schacht et al., 2019; H.
88 Wang et al., 2014) (Table 1). The treatment of wet-scavenging parameterizations is a key

89 factor affecting the model performance, which determines the uncertainties related to BC
90 particle removal (Kipling et al., 2013; Schacht et al., 2019; Q. Wang et al., 2014). The use of
91 emission inventories is another important factor that affects the simulation results (Dong et
92 al., 2019). The observations of BC that are used for model comparisons may be biased by a
93 [factor of 2](#) depending on the method used (Sinha et al., 2017; Sharma et al., 2017). There
94 are still large uncertainties regarding the sources of BC in the Arctic with respect to emission
95 sectors (anthropogenic sources and open biomass burning) and geospatial contributions
96 (Eckhardt et al., 2015).

97 The FLEXible PARTicle dispersion model (Flexpart) had been used to investigate the
98 transport pathways and source contributions of BC in the Arctic (Stohl et al., 1998, 2006,
99 2013). Of Flexpart model up to version 9, wet removal was treated considering below-cloud
100 and within-cloud scavenging processes (Hertel et al., 1995; McMahon and Denison, 1979),
101 which depends on cloud liquid water content, precipitation rate and the depth of the cloud.
102 However, clouds were parameterized based on relative humidity, clouds frequently
103 extended to the surface and at times no clouds could be found in grid cells, with unrealistic
104 precipitation (Grythe et al., 2017). Recently, version 10 of Flexpart had been developed in
105 which cloud is differentiated into liquid, solid, and mixed phase, the cloud distribution is
106 more consistent with the precipitation data (Grythe et al., 2017). This improvement in the
107 cloud distribution and phase leads to a more realistic distribution of below-cloud and in-
108 cloud scavenging events. In this study, we quantified region-separated sources of BC in the
109 Arctic in 2010 by using Flexpart v10.1. We first evaluated the model performance by
110 comparing the results with those based on observations at surface sites. The source
111 contributions of emission sectors and geospatial contributions were evaluated by
112 incorporating the Arctic BC footprint into the emission inventories.

Deleted: 30 %

114 2 Materials and methods

115 2.1 Transport model

116 The Flexpart model (version 10.1) was run in backward mode to simulate BC footprints in
117 the Arctic region. The calculation of wet deposition was improved compared with those in
118 previous versions because in-cloud scavenging and below-cloud scavenging of particles were
119 separately calculated (Grythe et al., 2017). In previous versions of Flexpart, in the in-cloud
120 scavenging scheme, the aerosol scavenging coefficient depended on the cloud water
121 content, which was calculated according to an empirical relationship with precipitation rate,
122 in which all aerosols had the same nucleation efficiency (Hertel et al., 1995 ; Stohl et al.,
123 2005). In the new version, the in-cloud scavenging scheme depends on the cloud water
124 phase (liquid, ice, or mixed phase). Aerosols were set as ice nuclei for ice clouds and as
125 cloud condensation nuclei for liquid-water clouds, respectively. For mixed-phase clouds, it
126 was assumed that 10 % of aerosols are ice nuclei and 90 % are cloud condensation nuclei,
127 because BC is much more efficiently removed in liquid water clouds than in ice clouds (Cozic
128 et al., 2007; Grythe et al., 2017). The below-cloud scavenging scheme can parameterize
129 below-cloud removal as a function of aerosol particle size, and precipitation type (snow or
130 rain) and intensity. The biases produced in simulations using the new scheme are therefore
131 smaller than those in the old scheme for wet deposition of aerosols, especially at high
132 latitudes (Grythe et al., 2017).

133 The Arctic region is defined as areas north of 66° N. The potential BC emission
134 sensitivities at two heights in the Arctic region, i.e., the surface (0–500 m) and [high altitudes](#)
135 (4750–5250 m), were simulated. The Flexpart outputs were set as gridded retention times.
136 We performed tests at 500, 2000, and 5000 m, and chose 500 m as the upper boundary
137 height of the model output. The model was driven with operational analytical data from the

Deleted: 5000 m

139 European Centre for Medium-Range Weather Forecasts (ECMWF) at a spatial resolution of
140 $1^\circ \times 1^\circ$ with 61 vertical levels. Temporally, ECMWF has a resolution of 3 h, with 6 h analysis
141 and 3 h forecast time steps. The simulation period was set at 60 days backward starting
142 from each month in 2010. The maximum lifetime of BC was set at 20 days because its
143 suspension time in the upper atmosphere during long-range transport is longer than that at
144 the surface level (Stohl et al., 2013). We implemented the wet deposition scheme in the
145 backward calculations, but it was not represented in the default setting (Flexpart v10.1,
146 <https://www.flexpart.eu/downloads>, obtained 10 April 2017).

147 The chemistry and microphysics could not be resolved by Flexpart. The model therefore
148 ignores hydrophobic to hydrophilic state changes and size changes of BC, and assumes that
149 all BC particles are aged hydrophilic particles. This may lead to an overestimation of BC
150 removal and hence force underestimation of simulated BC concentration, especially of fossil
151 fuel combustion sources where BC could be in the hydrophobic state for a few days. A
152 logarithmic size distribution of BC with a mean diameter of $0.16 \mu\text{m}$ and a standard
153 deviation of 1.96, in accordance with our ship observations in the Arctic, was used (Taketani
154 et al., 2016). The particle density was assumed to be 2000 kg m^{-3} , and 1 million
155 computational particles were randomly generated in the Arctic region for the backward
156 runs.

157 Four ground-based observations made during the period 2007–2011 were used to
158 validate the model performance. The potential BC emission sensitivity at 0–500 m above
159 ground level from a 0.1° grid centered at each site was simulated. Other model
160 parameterizations were consistent with those for the Arctic region, except that 200 000
161 computational particles were released.

162 2.2 Emission inventories

Deleted: life time

164 We focused on BC sources from anthropogenic emissions and open biomass burning. The
165 Hemispheric Transport of Air Pollution version 2 inventory (HTAP2) for 2010 was used for
166 monthly anthropogenic BC emissions (Janssens-Maenhout et al., 2015), which include
167 sectors from energy, industry, residential and transport. It is worth noting that the
168 residential sector includes not only combustions of fossil fuels, but also biofuels. However,
169 as it has been reported that BC emissions in Russia were underestimated in HTAP2, we used
170 the BC emissions reported by Huang et al. (2015) for Russia, in which the annual BC
171 emissions were 224 Gg yr⁻¹. For open biomass burning, we used the monthly BC emissions
172 from the Global Fire Emissions Database version 3 inventory (GFED3) (van der Werf et al.,
173 2010) for the purposes of intercomparison with other studies, as this version is widely used.
174 The term “open biomass burning” here indicates burning of biomass in the open field as is
175 determined by the remote sensing measurement basis, including forest, agricultural waste,
176 peat fires, grassland and savanna, woodland, deforestation and degradation, where biofuel
177 burning for residential use is not included. Geospatial distributions of emissions from
178 anthropogenic sources and open biomass burning in January and July are shown in Fig. S1.

179 2.3 Calculation of Arctic BC source contributions

180 The source contributions to Arctic BC were derived by incorporating the gridded
181 retention time into the column emission flux, which was derived from the emission
182 inventories in each grid. Calculations for anthropogenic sources and open biomass burning
183 were performed separately and the sum was used. For anthropogenic sources, the regions
184 were separated into North America and Canada (25–80° N, 50–170° W), Europe (30–80° N,
185 0–30° E), Russia (53–80° N, 30–180° E), East Asia (35–53° N, 75–150° E and 20–35° N, 100–
186 150° E), and others (the rest) (Fig. 1a). For open biomass burning sources, the regions were

187 separated into Alaska and Canada (50–75° N, 50–170° W), Siberia (50–75° N, 60–180° E),
188 and others (Fig. 1b).

189 2.3 Observations

190 BC levels simulated by Flexpart were compared with those based on surface observations
191 at four sites: Barrow, USA (156.6° W, 71.3° N, 11 m asl), Alert, Canada (62.3° W, 82.5° N,
192 210 m asl), Zeppelin, Norway (11.9° E, 78.9° N, 478 m asl), and Tiksi, Russia (128.9° E, 71.6°
193 N, 8 m asl). Aerosol light absorption was determined by using particle soot absorption
194 photometers (PSAPs) at Barrow, Alert, and Zeppelin, and an aethalometer at Tiksi. For PSAP
195 measurements, the equivalent BC values were derived using a mass absorption efficiency of
196 $10 \text{ m}^2 \text{ g}^{-1}$. The equivalent BC at Tiksi, which was determined with an aethalometer, was
197 obtained directly. These measurement data were obtained from the European Monitoring
198 and Evaluation Programme and World Data Centre for Aerosols database
199 (<http://ebas.nilu.no>) (Tørseth et al., 2012).

200 It is worth noting that uncertainties could be introduced by using different BC
201 measurement techniques. An evaluation of three methods for measuring BC at Alert,
202 Canada indicated that an average of the refractory BC determined with a single-particle soot
203 photometer (SP2) and elemental carbon (EC) determined from filter samples give the best
204 estimate of BC mass (Sharma et al., 2017). Xu et al. (2017) reported that the equivalent BC
205 determined with a PSAP was close to the average of the values for refractory BC and EC at
206 Alert. In this study, we consider that the equivalent BC values determined with a PSAP at
207 Barrow, Alert, and Zeppelin to be the best estimate. There may be uncertainties in the
208 equivalent BC observations performed with an aethalometer at Tiksi because of co-existing
209 particles such as light-absorptive organic aerosols, scattering particles, and dusts
210 (Kirchstetter et al., 2004; Lack and Langridge, 2013). Interference by the filter and

211 uncertainties in the mass absorption cross section could also contribute to the bias
212 observed in measurements made with an aethalometer at Tiksi.

213 **3 Results and discussion**

214 **3.1. Comparisons of simulations with BC observations at Arctic surface sites**

215 Flexpart generally reproduced the seasonal variations in BC at four Arctic sites well
216 [Pearson correlation coefficient (R) = 0.53–0.80, root-mean-square error (RMSE) = 15.1–56.8
217 ng m^{-3}] (Fig. 2). Winter maxima were observed for the four sites, while a secondary
218 elevation was observed for Alert and Tiksi. At Barrow, the observed high values of BC were
219 unintentionally excluded during data screening in the forest fire season in summer (Stohl et
220 al., 2013); the original observed BC is supposed to be higher as was reflected by the
221 simulation. This seasonality is probably related to relatively stronger transport to the Arctic
222 region in winter, accompanied by lower BC aging and inefficient removal, as simulated by
223 older versions of Flexpart (Eckhardt et al., 2015; Stohl et al., 2013).

224 From January to May at Barrow and Alert, the mean BC simulated by Flexpart v10.1 were
225 32.2 ng m^{-3} and 31.2 ng m^{-3} , respectively. Which was 46 % lower than the observations
226 (59.3 ng m^{-3} and 58.2 ng m^{-3} , respectively). This is probably related to the inadequate BC
227 emission in the inventory, although seasonal variations in residential heating are included in
228 HTAP2, which would reduce the simulation bias (Xu et al., 2017). Simulations by GEOS-Chem
229 using the same emission inventories also underestimated BC levels at Barrow and Alert
230 (Ikeda et al., 2017; Xu et al., 2017). The underestimation by Flexpart could also be partly
231 contributed by the assumption that all particles are hydrophilic, where the BC scavenging
232 could be overestimated. The corresponding uncertainties are larger in winter months, when
233 there are more sources from fossil fuel combustion.

234 At Zeppelin, the Flexpart-simulated BC (39.1 ng m^{-3} for annual mean) was 85 % higher
235 than the observed value (21.1 ng m^{-3} for annual mean), especially in winter (112% higher). It
236 has been reported that riming in mixed-phase clouds occurs frequently at Zeppelin (Qi et al.,
237 2017). During the riming process, BC particles act as ice particles and collide with the
238 relatively numerous water drops, which form frozen cloud droplets, and then snow is
239 precipitated. This results in relatively efficient BC scavenging (Hegg et al., 2011). Such a
240 process could not be dealt with by the model. At Tiksi, Flexpart underestimated BC (74.4 ng
241 m^{-3} for annual mean) in comparison with observation (104.2 ng m^{-3} for annual mean). Other
242 than the hydrophilic BC assumption and underestimated BC emission in the simulation as
243 the cases for Barrow and Alert, the observations at Tiksi by an aethalometer could
244 contain light-absorbing particles other than BC, resulting in higher observed
245 concentrations if compared with those obtained by SP2, EC and PSAP.

246 Anthropogenic emissions are the main sources of BC at the four Arctic sites from late
247 autumn to spring, whereas open biomass burning emissions make large contributions in
248 summer. From October to April, anthropogenic emissions accounted for 87–100 % of BC
249 sources at all the observation sites. At Barrow, open biomass burning accounted for 35–
250 78 % of BC in June–September (Fig. 2). There are large interannual variations in both
251 observed and simulated BC (Fig. S2). In June–August 2010, the mean contributions of open
252 biomass burning to BC were 6.3, 2.4, and 8.6 times those from anthropogenic sources at
253 Alert, Zeppelin, and Tiksi, respectively. In this study, we focused on BC in the Arctic region in
254 2010.

255 **3.2 Potential emission sensitivity of Arctic BC**

256 The potential emission sensitivities (footprint) of Arctic BC showed different patterns
257 with respect to altitude. The Arctic surface is sensitive to emissions at high latitudes ($>60^\circ$

258 N). Air masses stayed for over 60 s in each of the 1° grids from the eastern part of northern
259 Eurasia and the Arctic Ocean before being transported to the Arctic surface in the winter,
260 represented by January (Fig. 3a). In comparison, during the summer, represented by July, BC
261 at the Arctic surface was mainly affected by air masses that originated from the Arctic
262 Ocean and the Norwegian Sea (Fig. 3b). These results imply that local BC emissions within
263 the Arctic regions, although relatively weak compared with those from the mid-latitude
264 regions, could strongly affect Arctic air pollution. Local BC emissions are important in the
265 wintertime because the relatively stable boundary layer does not favor pollution dispersion.
266 Recent increases in anthropogenic emissions in the Arctic region, which have been caused
267 by the petroleum industry and development of the Northern Sea Route, are expected to
268 cause deterioration of air quality in the Arctic. Socio-economic developments in the Arctic
269 region would increase local BC emissions, and this will be a non-negligible issue in the future
270 (Roiger et al., 2015; Schmale et al., 2018).

271 BC at high altitudes in the Arctic is more sensitive to mid-latitude (30–60° N) emissions,
272 especially in wintertime. In January, air masses hovered over the Bering Sea and the North
273 Atlantic Ocean before arriving at the Arctic (Fig. 3c). A notable corridor at 30–50° N covering
274 Eurasia and the United States was the sensitive region that affected BC at high altitudes in
275 the Arctic in January. These results indicate that mid-latitude emissions, especially those
276 with relatively large strengths from East Asia, East America, and Europe, could alter the
277 atmospheric constituents at high altitudes in the Arctic. Central to east Siberia was the most
278 sensitive region for BC at high altitudes in the Arctic in July (Fig. 3d). These results suggest
279 that pollutants from frequent and extensive wildfires in Siberia in summer are readily
280 transported to high altitudes in the Arctic. Boreal fires are expected to occur more
281 frequently and over larger burning areas under future warming (Veira et al., 2016),

Deleted: (~ 5000 m)

283 therefore the atmospheric constituents and climate in the Arctic could undergo more rapid
284 changes.

285 **3.3 Seasonal variations and sources of Arctic surface BC**

286 Arctic surface BC showed clear seasonal variations, with a primary peak in winter–spring
287 (December–March, 61.8–82.8 ng m⁻³) and a secondary peak in summer (July, 52.7 ng m⁻³).
288 BC levels were relatively low in May–June (21.8–23.1 ng m⁻³) and September–November
289 (34.1–40.9 ng m⁻³) (Fig. 4a). This seasonality agrees with observations and simulations at
290 Alert, Tiksi, and Barrow if consider the unintentional data exclusion (Stohl et al., 2013), and
291 previous studies targeting the whole Arctic (Ikeda et al., 2017; Xu et al., 2017). Compared
292 with the study reported by Stohl et al. (2013), the current work using the new scheme
293 produced smaller discrepancies between the simulated data and observations. Although the
294 simulation periods (monthly means for 2007–2011 in this study and for 2008–2010 in the
295 old scheme) and the anthropogenic emission inventories (HTAP2 in this study and ECLIPSE4
296 in the previous study) are different, the new scheme shows potential for better representing
297 BC transport and removal processes in the Arctic.

298 The annual mean Arctic BC at the surface was estimated to be 48.2 ng m⁻³. From October
299 to April, anthropogenic sources accounted for 96–100 % of total BC at the Arctic surface.
300 Specifically, anthropogenic emissions from Russia accounted for 61–76 % of total BC in
301 October–May (56 % annually), and was the dominant sources of Arctic BC at the surface.
302 From an isentropic perspective, the meteorological conditions in winter favored the
303 transport of pollutants from northern Eurasia to the lower Arctic, along with diabatic cooling
304 and strong inversions (Klonecki et al., 2003). In comparison, open biomass burning from
305 boreal regions accounted for 56–85 % (75 % on average) of Arctic BC at the surface in
306 summer; open biomass burning emissions from North America and Canada accounted for

307 54 % of total Arctic surface BC in June, and those from Siberia accounted for 59–61 % in
308 July–August. Wildfires in the boreal forests in summer had a major effect on air quality in
309 the Arctic.

310 On an annual basis, anthropogenic sources and open biomass burning emissions
311 accounted for 82 % and 18 %, respectively, of total Arctic surface BC. In which, gas flaring
312 and residential burning (including burning of fossil fuels and biofuels) are accounting for
313 36 % (28–57 % in October–March) and 15 % (13–25 % in October–March), respectively (Fig.
314 5a-b). Our results support Stohl et al. (2013) that residential combustion emissions,
315 especially in winter are important sources of Arctic BC (Table 1). We estimated a
316 contribution of gas flaring to Arctic surface BC of 17.5 ng m^{-3} (36% of total). In comparison,
317 the value was estimated as 11.8 ng m^{-3} using an average Arctic surface BC of 28 ng m^{-3} and
318 a fraction from gas flaring of 42 % evaluated by earlier versions of Flexpart (Stohl et al.,
319 2013; Winiger et al., 2019). The different contribution could be partly attributed to the
320 difference in gas flaring emission inventory. BC emission from gas flaring in Russia by Huang
321 et al. (2015) was used in the current study, where total BC emission from gas flaring in
322 Russia in 2010 was ca. 81.1 kilotonne, which was larger than the estimate of ca. 64.9
323 kilotonne by GAINS inventory (Klimont et al., 2017) used by Stohl et al. (2013). Moreover,
324 Adopting ECLIPSEv5 inventory as was used by Winiger et al. (2019), we estimated that gas
325 flaring was contributing 14.4 ng m^{-3} to Arctic surface BC using Flexpart v10.1, a value 22 %
326 higher than those obtained using Flexpart v9. This difference could be attributed to the
327 improvement of the wet-scavenging scheme by Flexpart v10.1.

328 A recent study based on isotope observations at the Arctic sites and Flexpart v9.2
329 simulation suggested that open biomass burning, including open field burning and
330 residential biofuel burning, contributed 39 % of annual BC in 2011–2015 (Winiger et al.,

331 2019) (Table 1). In comparison, we estimated that residential burning and open biomass
332 burning together account for 33 % of total Arctic surface BC. As the residential burning in
333 our study includes burning of both biofuels and fossil fuels, our results indicated that
334 biomass burning has a relatively smaller contribution. Other than the differences in BC
335 removal treatment between different versions of the model, the contribution difference
336 could also be attributed to the different emission inventories and years (2010 versus 2011-
337 2015).

338 The geospatial contributions of anthropogenic sources and open biomass burning
339 emissions can be further illustrated by taking January and July as examples. In January, high
340 levels of anthropogenic emissions from Russia (contributing 64 % of Arctic surface BC),
341 Europe (18 %), and East Asia (9 %) were identified (Fig. 6a). Specifically, Yamalo-Nenets
342 Autonomous Okrug in Russia, which has the largest reserves of Russia's natural gas and oil
343 (Filimonova et al., 2018), was the most notable emission hotspot, which suggests gas-flaring
344 sources. The Komi Republic in Russia was also identified as a strong anthropogenic emitter
345 contributing to Arctic surface BC. These gas-flaring industrial regions in Russia (58–69° N,
346 68–81°E) together contributed 33 % and 31 % of Arctic surface BC for January and the
347 annual mean, respectively. Recently, Dong et al. (2019) evaluated BC emission inventories
348 using GEOS-Chem and proposed that using the inventory compiled by Huang et al. (2015)
349 for Russia, in which gas flaring accounted for 36 % of anthropogenic emissions, had no
350 prominent impact on the simulation performance in Russia and the Arctic. They suggested
351 that use of a new global inventory for BC emissions from natural gas flaring would improve
352 the model performance (Huang and Fu, 2016). These results suggest that inclusion of BC
353 emissions from gas flaring on the global scale is necessary for further BC simulations.

354 In Europe, a relatively high contribution of anthropogenic emissions to Arctic surface BC
355 in January was made by Poland (50–55° N, 15–24° E, contributing 4 % of Arctic surface BC)
356 because of relatively large emission fluxes in the region (Fig. S1a). Anthropogenic emissions
357 from East China, especially those north of ~33° N (33–43° N, 109–126° E), contributed
358 perceptibly (5 %) to Arctic surface BC.

359 In July, contributions from anthropogenic sources shrank to those from Yamalo-Nenets
360 Autonomous Okrug and Komi Republic in Russia, and contributed a lower fraction (3 % of
361 Arctic surface BC) (Fig. 6b). Few open biomass burning sources contributed in January (Fig.
362 6c), but contributions from open biomass burning to Arctic surface BC in July can be clearly
363 seen, mainly from the far east of Russia, Canada, and Alaska (Fig. 6d). Open biomass burning
364 emissions from Kazakhstan, southwest Russia, southern Siberia, and northeast China also
365 contributed to Arctic surface BC, although at relatively low strengths (Fig. 5d and Fig. S1d).
366 However, the contributions from open biomass burning could be higher, as the MODIS
367 burned area, the basis of GFED emission inventories, was underestimated for northern
368 Eurasia by 16 % (Zhu et al., 2017). Evangeliou et al. (2016) estimated a relatively high
369 transport efficiency of BC from open biomass burning emissions to the Arctic, which led to a
370 high contribution, i.e., 60 %, from such sources to BC deposition in the Arctic in 2010. A
371 recent study suggested that open fires burned in western Greenland in summer (31 July to
372 21 August 2017) could potentially alter the Arctic air composition and foster glacier melting
373 (Evangeliou et al., 2019). Although the footprint of Arctic surface BC showed a relatively
374 weak sensitivity to areas such as forests and tundra, in the boreal regions, pollutants from
375 boreal wildfires could have greater effects on the Arctic air composition in summer under
376 future warming scenarios (Veira et al., 2016).

377 **3.4 Sources of Arctic BC at high altitudes**

378 Arctic BC levels at high altitudes showed the highest levels in spring (March–April, 40.5–
379 53.9 ng m⁻³), followed by those in late autumn to early winter (November–January, 36.5–
380 40.0 ng m⁻³), and summer (July–August, 33.0–39.0 ng m⁻³) (Fig. 4c). The annual mean Arctic
381 BC at high altitudes was estimated to be 35.2 ng m⁻³, which is ca. 73 % of those at the
382 surface. Such a vertical profile is in accordance with those based on aircraft measurements
383 over the High Canadian Arctic (Schulz et al., 2019). Similarly to the case for the surface,
384 anthropogenic sources dominated by residential sectors, transport, industry and energy
385 (excluding gas flaring), accounted for 94–100 % of Arctic BC at high altitudes in October–
386 May (Figs. 4c, 5c). East Asia accounted for 34–65 % of the total BC in October–May (40 %
387 annually). In comparison, using the Community Atmosphere Model version 5 driven by the
388 NASA Modern Era Retrospective-Analysis for Research and Applications reanalysis data and
389 the IPCC AR5 year 2000 BC emission inventory, H. Wang et al. (2014) found that East Asia
390 accounted for 23% of BC burden in the Arctic for 1995–2005. In summer, open biomass
391 burning in the boreal regions accounted for 40–72 % (57 % on average) of Arctic BC at high
392 altitudes, similar to the source contributions to Arctic surface BC. Specifically, open biomass
393 burning sources from Siberia accounted for 40–42 % of Arctic BC at high altitudes in July–
394 August. Annually, anthropogenic sources and open biomass burning accounted for 83 % (in
395 which residential sources accounted for 34%) and 17 %, respectively, of total Arctic BC at
396 high altitudes (Figs. 4d, 5d).

397 Further investigations of geospatial contributions to Arctic BC at high altitudes in January
398 and July provided more details regarding BC sources. In January, the main anthropogenic BC
399 source in East Asia covered a wide range in China (Fig. 7a). Not only east and northeast
400 China, but also southwest China (Sichuan and Guizhou provinces) were the major
401 anthropogenic sources of Arctic BC at high altitudes. In July, anthropogenic sources made a

Deleted: (4750–4250 m)

403 relatively weak contribution to Arctic BC at high altitudes. The regions that were sources of
404 open biomass burning contributions to Arctic BC at high altitudes were mainly the far east of
405 Siberia, Kazakhstan, central Canada, and Alaska, i.e., similar to the sources of Arctic surface
406 BC. Unlike Arctic surface BC, for which the dominant source regions are at high latitudes in
407 both winter and summer, Arctic BC at high altitudes mainly originates from mid-latitude
408 regions (Figs. 6 and 7). In terms of transport pathways, air masses could be uplifted at low-
409 to-mid latitudes and transported to the Arctic (Stohl, 2006). Further investigations are
410 needed to obtain more details of the transport processes.

411 **3.5 Comparison of Flexpart and GEOS-Chem simulations of BC sources**

412 Data for BC sources simulated with Flexpart were compared with those obtained with
413 GEOS-Chem (Ikeda et al., 2017), which is an Eulerian atmospheric transport model, using the
414 same emission inventories. The simulated seasonal variations in Arctic BC levels and source
415 contributions obtained with Flexpart agreed well with those obtained with GEOS-Chem (Fig.
416 S3). The annual mean BC levels at the Arctic surface obtained by Flexpart and GEOS-Chem
417 simulations were 48 and 70 ng m⁻³, respectively; the high-altitude values simulated by
418 Flexpart and GEOS-Chem were 35 and 38 ng m⁻³, respectively. The magnitude difference
419 between the BC levels at the Arctic surface could be related to meteorology. ECMWF ERA-
420 Interim data were used as the input for the Flexpart simulation, whereas the GEOS-Chem
421 simulation was driven by assimilated meteorological data from the Goddard Earth
422 Observation System (GEOS-5).

423 The treatments of the BC removal processes could also lead to different simulation
424 results, depending on the model. In terms of BC loss processes, dry and wet depositions
425 were the removal pathways, depending on the particle size and density, in Flexpart. The
426 treatment of meteorology, especially cloud water and precipitation, would therefore affect

427 the uncertainties of the simulations. In Flexpart version 10.1, BC particles are separately
428 parameterized as ice nuclei for ice clouds, cloud condensation nuclei for liquid-water clouds,
429 and 90 % as cloud condensation nuclei for mixed-phase clouds. The separation of mixed-
430 phase clouds is realistic, as 77 % of in-cloud scavenging processes occurred in the mixed
431 phase over a 90 day period starting from December 2006 (Grythe et al., 2017).

432 In GEOS-Chem simulations, the BC aging was parameterized based on the number
433 concentration of OH radicals (Liu et al., 2011). The BC was assumed to be hydrophilic in
434 liquid clouds ($T \geq 258$ K) and hydrophobic when serving as ice nuclei in ice clouds ($T < 258$ K)
435 (Wang et al., 2011), with modifications because the scavenging rate of hydrophobic BC was
436 reduced to 5 % of water-soluble aerosols for liquid clouds (Bourgeois and Bey, 2011). Such a
437 treatment is expected to improve the simulation accuracy (Ikeda et al., 2017).

438 In Lagrangian models, the trajectories of particles are computed by following the
439 movement of air masses with no numerical diffusion, although some artificial numerical
440 errors could be generated from stochastic differential equations (Ramli and Esler, 2016). As
441 a result, long-range transport processes can be well simulated (Stohl, 2006; Stohl et al.,
442 2013). In comparison, Eulerian chemical transport models such as GEOS-Chem have the
443 advantage of simulating non-linear processes on the global scale, which enables treatment
444 of the BC aging processes (coating with soluble components) (Bey et al, 2001; Eastham et
445 al., 2018). However, with GEOS-Chem, the capture of intercontinental pollution plumes is
446 difficult because of numerical plume dissipation (Rastigejev et al., 2010). Nevertheless, the
447 agreement between the Flexpart and GEO-Chem simulations of BC source contributions
448 indicates improved reliability of evaluated source contributions to Arctic BC.

449 **4 Conclusions**

450 The source contributions to Arctic BC were investigated by using a Flexpart (version 10.1)
451 transport model that incorporated emission inventories. Flexpart-simulated BC data agreed
452 well with observations at Arctic sites, i.e., Barrow, Alert, Zeppelin, and Tiksi. The source
453 regions and source sectors of BC at the surface and high altitudes over a wide region in the
454 Arctic north of 66° N were simulated. BC at the Arctic surface was sensitive to local
455 emissions and those from nearby Nordic countries (>60° N). These results emphasize the
456 role of anthropogenic emissions such as gas flaring and development of the Northern Sea
457 Route in affecting air quality and climate change in the Arctic. Anthropogenic emissions in
458 the northern regions of Russia were the main source (56 %) of Arctic surface BC annually. In
459 contrast, BC in the Arctic at high altitudes was sensitive to mid-latitude emissions (30–60°
460 N). Although they are geospatially far from the Arctic, anthropogenic emissions in East Asia
461 made a notable (40 %) contribution to BC in the Arctic at high altitudes annually. Open
462 biomass burning emissions, which were mainly from Siberia, Alaska, and Canada, were
463 important in summer, contributing 56–85 % of BC at the Arctic surface, and 40–72 % at
464 Arctic high altitudes. Future increases in wildfires as a result of global warming could
465 therefore increase the air pollution level during the Arctic summer. This study clarifies the
466 source regions and sectors of BC in the Arctic. This information is fundamental for
467 understanding and tackling air pollution and climate change in the region.

468
469 *Data Availability.* The data set for simulated footprint and BC source contributions is
470 available on request to the corresponding author.

471

472 *Author contributions.* CZ and YK designed the study. CZ, MT, and IP optimized the Flexpart
473 model. CZ performed Flexpart model simulations, conducted analyses, and wrote the

Deleted: (~ 5000 m)

475 manuscript. KI and HT provided data for GEOS-Chem simulations and site observations. All
476 authors made comments that improved the paper.

477

478 *Competing interests.* The authors declare that they have no conflict of interest.

479

480 *Financial Support.* This study was supported by the Environmental Research and Technology
481 Development Fund (2-1505) of the Ministry of the Environment, Japan.

482

483 *Acknowledgment.* We acknowledge staffs from the following university and agencies for BC
484 observational data: Barrow and Tiksi sites are operated by National Oceanic and

485 Atmospheric Administration; Zeppelin site is operated by Stockholm University; and Alert

486 site is operated by Environment and Climate Change Canada. We are grateful to [Chandra](#)

487 [Mouli Pavuluri \(Tianjin University\)](#) and an anonymous reviewer for the comments. We thank

488 Helen McPherson, PhD, from Edanz Group (www.edanzediting.com/ac) for editing a draft of

489 this manuscript.

490

491 **References**

492 AMAP Assessment 2015: Black carbon and ozone as Arctic climate forcers, Arctic Monitoring
493 and Assessment Programme (AMAP), Oslo, Norway, 2015.

494 Bey, I., Jacob, D. J., Yantosca, R. M., Logan, J. A., Field, B. D., Fiore, A. M., Li, Q. B., Liu, H. G.

495 Y., Mickley, L. J., and Schultz, M. G.: Global modeling of tropospheric chemistry with

496 assimilated meteorology: Model description and evaluation, *J Geophys Res-Atmos*, 106,

497 23073-23095, doi:10.1029/2001jd000807, 2001.

498 Bourgeois, Q. and Bey, I.: Pollution transport efficiency toward the Arctic: sensitivity to

499 aerosol scavenging and source regions, *J. Geophys. Res.*, 116, D08213,

500 doi:10.1029/2010JD015096, 2011.

Deleted: two

Deleted: s

503 Brock, C. A., Cozic, J., Bahreini, R., Froyd, K. D., Middlebrook, A. M., McComiskey, A.,
504 Brioude, J., Cooper, O. R., Stohl, A., Aikin, K. C., de Gouw, J. A., Fahey, D. W., Ferrare, R.
505 A., Gao, R. S., Gore, W., Holloway, J. S., Hubler, G., Jefferson, A., Lack, D. A., Lance, S.,
506 Moore, R. H., Murphy, D. M., Nenes, A., Novelli, P. C., Nowak, J. B., Ogren, J. A., Peischl, J.,
507 Pierce, R. B., Pilewskie, P., Quinn, P. K., Ryerson, T. B., Schmidt, K. S., Schwarz, J. P.,
508 Sodemann, H., Spackman, J. R., Stark, H., Thomson, D. S., Thornberry, T., Veres, P., Watts,
509 L. A., Warneke, C., and Wollny, A. G.: Characteristics, sources, and transport of aerosols
510 measured in spring 2008 during the aerosol, radiation, and cloud processes affecting
511 Arctic Climate (ARCPAC) Project, *Atmospheric Chemistry and Physics*, 11, 2423-2453,
512 doi:10.5194/acp-11-2423-2011, 2011.

513 Cohen, J., Screen, J. A., Furtado, J. C., Barlow, M., Whittleston, D., Coumou, D., Francis, J.,
514 Dethloff, K., Entekhabi, D., Overland, J., and Jones, J.: Recent Arctic amplification and
515 extreme mid-latitude weather, *Nature Geoscience*, 7, 627-637, doi:10.1038/Ngeo2234,
516 2014.

517 Cozic, J., Verheggen, B., Mertes, S., Connolly, P., Bower, K., Petzold, A., Baltensperger, U.,
518 and Weingartner, E.: Scavenging of black carbon in mixed phase clouds at the high alpine
519 site Jungfraujoch, *Atmos. Chem. Phys.*, 7, 1797-1807, doi:10.5194/acp-7-1797-2007,
520 2007.

521 Dong, X., Zhu, Q., Fu, J. S., Huang, K., Tan, J., and Tipton, M.: Evaluating recent updated black
522 carbon emissions and revisiting the direct radiative forcing in Arctic, *Geophysical*
523 *Research Letters*, 46, 3560– 3570. doi:10.1029/2018GL081242, 2019.

524 Eastham, S. D., Long, M. S., Keller, C. A., Lundgren, E., Yantosca, R. M., Zhuang, J. W., Li, C.,
525 Lee, C. J., Yannetti, M., Auer, B. M., Clune, T. L., Kouatchou, J., Putman, W. M., Thompson,
526 M. A., Trayanov, A. L., Molod, A. M., Martin, R. V., and Jacob, D. J.: GEOS-Chem High
527 Performance (GCHP v11-02c): a next-generation implementation of the GEOS-Chem
528 chemical transport model for massively parallel applications, *Geosci Model Dev*, 11,
529 2941-2953, doi:10.5194/gmd-11-2941-2018, 2018.

530 Eckhardt, S., Quennehen, B., Olivie, D. J. L., Berntsen, T. K., Cherian, R., Christensen, J. H.,
531 Collins, W., Crepinsek, S., Daskalakis, N., Flanner, M., Herber, A., Heyes, C., Hodnebrog,
532 O., Huang, L., Kanakidou, M., Klimont, Z., Langner, J., Law, K. S., Lund, M. T., Mahmood,
533 R., Massling, A., Myriokefalitakis, S., Nielsen, I. E., Nojgaard, J. K., Quaas, J., Quinn, P. K.,
534 Raut, J. C., Rumbold, S. T., Schulz, M., Sharma, S., Skeie, R. B., Skov, H., Uttal, T., von

- 535 Salzen, K., and Stohl, A.: Current model capabilities for simulating black carbon and
536 sulfate concentrations in the Arctic atmosphere: a multi-model evaluation using a
537 comprehensive measurement data set, *Atmospheric Chemistry and Physics*, 15, 9413-
538 9433, doi:10.5194/acp-15-9413-2015, 2015.
- 539 Evangeliou, N., Balkanski, Y., Hao, W. M., Petkov, A., Silverstein, R. P., Corley, R., Nordgren,
540 B. L., Urbanski, S. P., Eckhardt, S., Stohl, A., Tunved, P., Crepinsek, S., Jefferson, A.,
541 Sharma, S., Nojgaard, J. K., and Skov, H.: Wildfires in northern Eurasia affect the budget of
542 black carbon in the Arctic - a 12-year retrospective synopsis (2002-2013), *Atmospheric
543 Chemistry and Physics*, 16, 7587-7604, doi:10.5194/acp-16-7587-2016, 2016.
- 544 Evangeliou, N., Kylling, A., Eckhardt, S., Myroniuk, V., Stebel, K., Paugam, R., Zibitsev, S., and
545 Stohl, A.: Open fires in Greenland in summer 2017: transport, deposition and radiative
546 effects of BC, OC and BrC emissions, *Atmospheric Chemistry and Physics*, 19, 1393-1411,
547 doi:10.5194/acp-19-1393-2019, 2019.
- 548 Filimonova, I. V., Komarova, A. V., Eder, L. V., and Provornaya, I. V.: State instruments for the
549 development stimulation of Arctic resources regions, *IOP Conference Series: Earth and
550 Environmental Science*, 193, 012069, doi:10.1088/1755-1315/193/1/012069, 2018.
- 551 Garrett, T. J., Brattstrom, S., Sharma, S., Worthy, D. E. J., and Novelli, P.: The role of
552 scavenging in the seasonal transport of black carbon and sulfate to the Arctic,
553 *Geophysical Research Letters*, 38, L16805, doi:10.1029/2011gl048221, 2011.
- 554 Grythe, H., Kristiansen, N. I., Zwaafink, C. D. G., Eckhardt, S., Strom, J., Tunved, P., Krejci, R.,
555 and Stohl, A.: A new aerosol wet removal scheme for the Lagrangian particle model
556 FLEXPART v10, *Geosci Model Dev*, 10, 1447-1466, doi:10.5194/gmd-10-1447-2017, 2017.
- 557 Hegg, D. A., Clarke, A. D., Doherty, S. J., and Ström, J.: Measurements of black carbon
558 aerosol washout ratio on Svalbard, *Tellus B*, 63, 891-900, doi:10.1111/j.1600-
559 0889.2011.00577.x, 2011.
- 560 Hertel, O., Christensen, J. Runge, E. H., Asman, W. A. H., Berkowicz, R., Hovmand, M. F., and
561 Hov, O.: Development and testing of a new variable scale air pollution model – ACDEP,
562 *Atmos. Environ.*, 29, 1267-1290, 1995.
- 563 Hirdman, D., Burkhardt, J. F., Sodemann, H., Eckhardt, S., Jefferson, A., Quinn, P. K., Sharma,
564 S., Strom, J., and Stohl, A.: Long-term trends of black carbon and sulphate aerosol in the
565 Arctic: changes in atmospheric transport and source region emissions, *Atmospheric
566 Chemistry and Physics*, 10, 9351-9368, doi:10.5194/acp-10-9351-2010, 2010.

- 567 Huang, K., and Fu, J. S.: A global gas flaring black carbon emission rate dataset from 1994 to
568 2012, *Scientific Data*, 3, 160104. doi:10.1038/sdata.2016.104, 2016.
- 569 Huang, K., Fu, J. S., Prikhodko, V. Y., Storey, J. M., Romanov, A., Hodson, E. L., Cresko, J.,
570 Morozova, I., Ignatieva, Y., and Cabaniss, J.: Russian anthropogenic black carbon:
571 Emission reconstruction and Arctic black carbon simulation, *J Geophys Res-Atmos*, 120,
572 11306-11333, doi:10.1002/2015jd023358, 2015.
- 573 Ikeda, K., Tanimoto, H., Sugita, T., Akiyoshi, H., Kanaya, Y., Zhu, C. M., and Taketani, F.:
574 Tagged tracer simulations of black carbon in the Arctic: transport, source contributions,
575 and budget, *Atmospheric Chemistry and Physics*, 17, 10515-10533, doi:10.5194/acp-17-
576 10515-2017, 2017.
- 577 Janssens-Maenhout, G., Crippa, M., Guizzardi, D., Dentener, F., Muntean, M., Pouliot, G.,
578 Keating, T., Zhang, Q., Kurokawa, J., Wankmüller, R., Denier van der Gon, H., Kuenen, J. J.
579 P., Klimont, Z., Frost, G., Darras, S., Koffi, B., and Li, M.: HTAP_v2.2: a mosaic of regional
580 and global emission grid maps for 2008 and 2010 to study hemispheric transport of air
581 pollution, *Atmos. Chem. Phys.*, 15, 11411-11432, doi:10.5194/acp-15-11411-2015, 2015.
- 582 Keegan, K. M., Albert, M. R., McConnell, J. R., and Baker, I.: Climate change and forest fires
583 synergistically drive widespread melt events of the Greenland Ice Sheet, *P Natl Acad Sci*
584 *USA*, 111, 7964-7967, doi:10.1073/pnas.1405397111, 2014.
- 585 Kipling, Z., Stier, P., Schwarz, J. P., Perring, A. E., Spackman, J. R., Mann, G. W., Johnson, C.
586 E., and Telford, P. J.: Constraints on aerosol processes in climate models from vertically-
587 resolved aircraft observations of black carbon, *Atmos. Chem. Phys.*, 13, 5969-5986,
588 doi:10.5194/acp-13-5969-2013, 2013.
- 589 Kirchstetter, T. W., Novakov, T., and Hobbs, P. V.: Evidence that the spectral dependence of
590 light absorption by aerosols is affected by organic carbon, *J Geophys Res-Atmos*, 109,
591 D21208, doi:10.1029/2004jd004999, 2004.
- 592 Klimont, Z., Kupiainen, K., Heyes, C., Purohit, P., Cofala, J., Rafaj, P., Borken-Kleefeld, J., and
593 Schöpp, W.: Global anthropogenic emissions of particulate matter including black carbon,
594 *Atmos. Chem. Phys.*, 17, 8681-8723, doi:10.5194/acp-17-8681-2017, 2017.
- 595 Klonecki, A., Hess, P., Emmons, L., Smith, L., Orlando, J., and Blake, D.: Seasonal changes in
596 the transport of pollutants into the Arctic troposphere-model study, *J Geophys Res-*
597 *Atmos*, 108, 8367, doi:10.1029/2002jd002199, 2003.

- 598 Koch, D., and Hansen, J.: Distant origins of Arctic black carbon: A Goddard Institute for Space
599 Studies ModelE experiment, *J Geophys Res-Atmos*, 110, D04204,
600 doi:10.1029/2004jd005296, 2005.
- 601 Koch, D., Schmidt, G. A., and Field, C. V.: Sulfur, sea salt, and radionuclide aerosols in GISS
602 ModelE, *J. Geophys. Res.*, 111, D06206, doi:10.1029/2004jd005550, 2006.
- 603 Lack, D. A., and Langridge, J. M.: On the attribution of black and brown carbon light
604 absorption using the Angstrom exponent, *Atmospheric Chemistry and Physics*, 13,
605 10535–10543, doi:10.5194/acp-13-10535-2013, 2013.
- 606 Law, K. S., and Stohl, A.: Arctic air pollution: Origins and impacts, *Science*, 315, 1537–1540,
607 doi:10.1126/science.1137695, 2007.
- 608 Liu, J., Fan, S., Horowitz, L. W., and Levy II, H.: Evaluation of factors controlling long-range
609 transport of black carbon to the Arctic, *J. Geophys. Res.*, 116, D00A14,
610 doi:10.1029/2010JD015145, 2011.
- 611 Liu, D., Quennehen, B., Darbyshire, E., Allan, J. D., Williams, P. I., Taylor, J. W., Bauguitte, S. J.
612 B., Flynn, M. J., Lowe, D., Gallagher, M. W., Bower, K. N., Choulaton, T. W., and Coe, H.:
613 The importance of Asia as a source of black carbon to the European Arctic during
614 springtime 2013, *Atmospheric Chemistry and Physics*, 15, 11537–11555, doi:10.5194/acp-
615 15-11537-2015, 2015.
- 616 Ma, P.-L., Rasch, P. J., Wang, H., Zhang, K., Easter, R. C., Tilmes, S., Fast, J. D., Liu, X., Yoon, J.-
617 H., and Lamarque, J.-F.: The role of circulation features on black carbon transport into the
618 Arctic in the Community Atmosphere Model version 5 (CAM5), *J. Geophys. Res.-Atmos.*,
619 118, 4657–4669, doi:10.1002/jgrd.50411, 2013.
- 620 McMahon, T. A. and Denison, P. J.: Empirical atmospheric deposition parameters – a survey,
621 *Atmos. Environ.*, 13, 571–585, doi:10.1016/0004-6981(79)90186-0, 1979.
- 622 Najafi, M. R., Zwiers, F. W., and Gillett, N. P.: Attribution of Arctic temperature change to
623 greenhouse-gas and aerosol influences, *Nature Climate Change*, 5, 246-249,
624 doi:10.1038/Nclimate2524, 2015.
- 625 Park, R. J., Jacob, D. J., Palmer, P. I., Clarke, A. D., Weber, R. J., Zondlo, M. A., Eisele, F. L.,
626 Bandy, A. R., Thornton, D. C., Sachse, G. W., and Bond, T. C.: Export efficiency of black
627 carbon aerosol in continental outflow: Global implications, *J Geophys Res-Atmos*, 110,
628 D11205, doi:10.1029/2004jd005432, 2005.

- 629 Qi, L., Li, Q. B., Henze, D. K., Tseng, H. L., and He, C. L.: Sources of springtime surface black
630 carbon in the Arctic: an adjoint analysis for April 2008, *Atmospheric Chemistry and
631 Physics*, 17, 9697–9716, doi:10.5194/acp-17-9697-2017, 2017.
- 632 Quinn, P. K., Bates, T. S., Baum, E., Doubleday, N., Fiore, A. M., Flanner, M., Fridlind, A.,
633 Garrett, T. J., Koch, D., Menon, S., Shindell, D., Stohl, A., and Warren, S. G.: Short-lived
634 pollutants in the Arctic: their climate impact and possible mitigation strategies,
635 *Atmospheric Chemistry and Physics*, 8, 1723–1735, doi:10.5194/acp-8-1723-2008, 2008.
- 636 Ramli, H. M. and Esler, J. G.: Quantitative evaluation of numerical integration schemes for
637 Lagrangian particle dispersion models, *Geosci. Model Dev.*, 9, 2441–2457,
638 doi:10.5194/gmd-9-2441-2016, 2016.
- 639 Rastigejev, Y., Park, R., Brenner, M., and Jacob, D.: Resolving intercontinental pollution
640 plumes in global models of atmospheric transport, *J. Geophys. Res.*, 115, D02302,
641 doi:10.1029/2009JD012568, 2010.
- 642 Roiger, A., Thomas, J. L., Schlager, H., Law, K. S., Kim, J., Schafler, A., Weinzierl, B.,
643 Dahloktter, F., Krisch, I., Marelle, L., Minikin, A., Raut, J. C., Reiter, A., Rose, M., Scheibe,
644 M., Stock, P., Baumann, R., Bouapar, I., Clerbaux, C., George, M., Onishi, I., and Flemming,
645 J.: Quantifying emerging local anthropogenic emissions in the Arctic region: The ACCESS
646 aircraft campaign experiment, *B. Am. Meteorol. Soc.*, 96, 441–460, doi:10.1175/Bams-D-
647 13-00169.1, 2015.
- 648 Sand, M., Berntsen, T. K., von Salzen, K., Flanner, M. G., Langner, J., and Victor, D. G.:
649 Response of Arctic temperature to changes in emissions of short-lived climate forcers,
650 *Nature Climate Change*, 6, 286–289, doi:10.1038/Nclimate2880, 2016.
- 651 Schacht, J., Heinold, B., Quaas, J., Backman, J., Cherian, R., Ehrlich, A., Herber, A., Huang, W.
652 T. K., Kondo, Y., Massling, A., Sinha, P. R., Weinzierl, B., Zanatta, M., and Tegen, I.: The
653 importance of the representation of air pollution emissions for the modeled distribution
654 and radiative effects of black carbon in the Arctic, *Atmos. Chem. Phys.*, 19, 11159–11183,
655 doi:10.5194/acp-19-11159-2019, 2019.
- 656 Schmale, J., Arnold, S. R., Law, K. S., Thorp, T., Anenberg, S., Simpson, W. R., Mao, J., and
657 Pratt, K. A.: Local Arctic Air Pollution: A Neglected but Serious Problem, *Earths Future*, 6,
658 1385–1412, doi:10.1029/2018ef000952, 2018.
- 659 Schulz, H., Zanatta, M., Bozem, H., Leaitch, W. R., Herber, A. B., Burkart, J., Willis, M. D.,
660 Kunkel, D., Hoor, P. M., Abbatt, J. P. D., and Gerdes, R.: High Arctic aircraft measurements

- 661 characterising black carbon vertical variability in spring and summer, *Atmospheric*
662 *Chemistry and Physics*, 19, 2361–2384, doi:10.5194/acp-19-2361-2019, 2019.
- 663 Sharma, S., Leaitch, W. R., Huang, L., Veber, D., Kolonjari, F., Zhang, W., Hanna, S. J.,
664 Bertram, A. K., and Ogren, J. A.: An evaluation of three methods for measuring black
665 carbon in Alert, Canada, *Atmospheric Chemistry and Physics*, 17, 15225–15243,
666 doi:10.5194/acp-17-15225-2017, 2017.
- 667 Shaw, G. E.: The arctic haze phenomenon, *B Am Meteorol Soc*, 76, 2403–2413, 1995.
- 668 Shen, Z. Y., Ming, Y., Horowitz, L. W., Ramaswamy, V., and Lin, M. Y.: On the seasonality of
669 Arctic black carbon, *J. Climate*, 30, 4429–4441, doi:10.1175/Jcli-D-16-0580.1, 2017.
- 670 Shindell, D. T., Chin, M., Dentener, F., Doherty, R. M., Faluvegi, G., Fiore, A. M., Hess, P.,
671 Koch, D. M., MacKenzie, I. A., Sanderson, M. G., Schultz, M. G., Schulz, M., Stevenson, D.
672 S., Teich, H., Textor, C., Wild, O., Bergmann, D. J., Bey, I., Bian, H., Cuvelier, C., Duncan, B.
673 N., Folberth, G., Horowitz, L. W., Jonson, J., Kaminski, J. W., Marmor, E., Park, R., Pringle,
674 K. J., Schroeder, S., Szopa, S., Takemura, T., Zeng, G., Keating, T. J., and Zuber, A.: A multi-
675 model assessment of pollution transport to the Arctic, *Atmos. Chem. Phys.*, 8, 5353–5372,
676 doi:10.5194/acp-8-5353-2008, 2008.
- 677 Sinha, P. R., Kondo, Y., Koike, M., Ogren, J. A., Jefferson, A., Barrett, T. E., Sheesley, R. J.,
678 Ohata, S., Moteki, N., Coe, H., Liu, D., Irwin, M., Tunved, P., Quinn, P. K., and Zhao, Y.:
679 Evaluation of ground-based black carbon measurements by filter-based photometers at
680 two Arctic sites, *J Geophys Res-Atmos*, 122, 3544–3572, doi:10.1002/2016jd025843,
681 2017.
- 682 Stohl, A., Forster, C., Frank, A., Seibert, P., and Wotawa, G.: Technical note: The Lagrangian
683 particle dispersion model FLEXPART version 6.2, *Atmos. Chem. Phys.*, 5, 2461–2474,
684 doi:10.5194/acp-5-2461-2005, 2005.
- 685 Stohl, A.: Characteristics of atmospheric transport into the Arctic troposphere, *J Geophys*
686 *Res-Atmos*, 111, D11306, doi:10.1029/2005jd006888, 2006.
- 687 Stohl, A., Hittenberger, M., and Wotawa, G.: Validation of the Lagrangian particle dispersion
688 model FLEXPART against large-scale tracer experiment data, *Atmos Environ*, 32, 4245–
689 4264, doi:10.1016/S1352-2310(98)00184-8, 1998.
- 690 Stohl, A., Klimont, Z., Eckhardt, S., Kupiainen, K., Shevchenko, V. P., Kopeikin, V. M., and
691 Novigatsky, A. N.: Black carbon in the Arctic: the underestimated role of gas flaring and

- 692 residential combustion emissions, *Atmospheric Chemistry and Physics*, 13, 8833-8855,
693 doi:10.5194/acp-13-8833-2013, 2013.
- 694 Taketani, F., Miyakawa, T., Takashima, H., Komazaki, Y., Pan, X., Kanaya, Y., and Inoue, J.:
695 Shipborne observations of atmospheric black carbon aerosol particles over the Arctic
696 Ocean, Bering Sea, and North Pacific Ocean during September 2014, *J Geophys Res-*
697 *Atmos*, 121, 1914-1921, doi:10.1002/2015jd023648, 2016.
- 698 Tietze, K., Riedi, J., Stohl, A., and Garrett, T. J.: Space-based evaluation of interactions
699 between aerosols and low-level Arctic clouds during the Spring and Summer of 2008,
700 *Atmospheric Chemistry and Physics*, 11, 3359-3373, doi:10.5194/acp-11-3359-2011,
701 2011.
- 702 Tilling, R. L., Ridout, A., Shepherd, A., and Wingham, D. J.: Increased Arctic sea ice volume
703 after anomalously low melting in 2013, *Nature Geoscience*, 8, 643-646,
704 doi:10.1038/Ngeo2489, 2015.
- 705 Tørseth, K., Aas, W., Breivik, K., Fjæraa, A. M., Fiebig, M., Hjellbrekke, A. G., Lund Myhre, C.,
706 Solberg, S., and Yttri, K. E.: Introduction to the European Monitoring and Evaluation
707 Programme (EMEP) and observed atmospheric composition change during 1972–2009,
708 *Atmos. Chem. Phys.*, 12, 5447–5481, doi:10.5194/acp-12-5447-2012, 2012.
- 709 Trusel, L. D., Das, S. B., Osman, M. B., Evans, M. J., Smith, B., Fettweis, X., McConnell, J. R.,
710 Noel, B. P. Y., and van den Broeke, M. R.: Nonlinear rise in Greenland runoff in response
711 to post-industrial Arctic warming, *Nature*, 564, 104-108, doi:10.1038/s41586-018-0752-4,
712 2018.
- 713 van der Werf, G. R., Randerson, J. T., Giglio, L., Collatz, G. J., Mu, M., Kasibhatla, P. S.,
714 Morton, D. C., DeFries, R. S., Jin, Y., and van Leeuwen, T. T.: Global fire emissions and the
715 contribution of deforestation, savanna, forest, agricultural, and peat fires (1997–2009),
716 *Atmospheric Chemistry and Physics*, 10, 11707-11735, doi:10.5194/acp-10-11707-2010,
717 2010.
- 718 Veira, A., Lasslop, G., and Kloster, S.: Wildfires in a warmer climate: Emission fluxes,
719 emission heights, and black carbon concentrations in 2090-2099, *J Geophys Res-Atmos*,
720 121, 3195-3223, doi:10.1002/2015jd024142, 2016.
- 721 Wang, H., Rasch, P. J., Easter, R. C., Singh, B., Zhang, R., Ma, P. L., Qian, Y., and Beagley, N.:
722 Using an explicit emission tag- ging method in global modeling of source-receptor

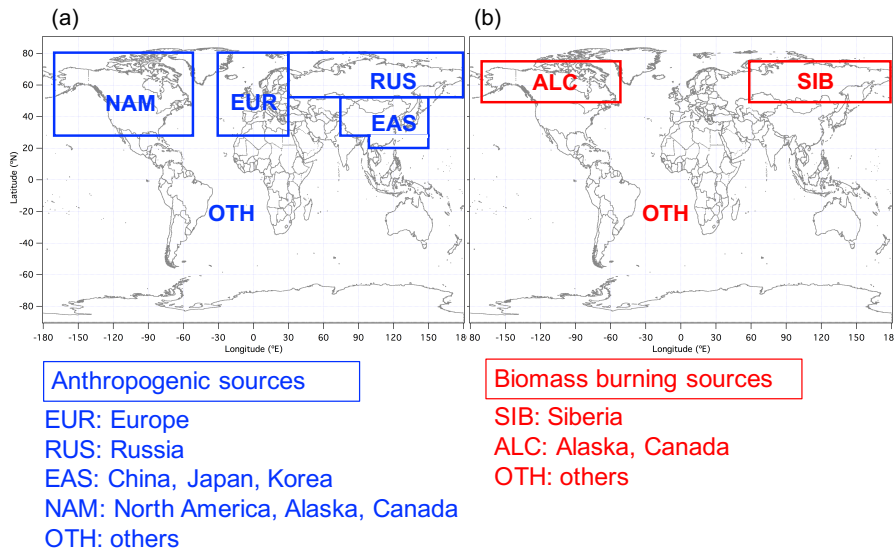
- 723 relationships for black carbon in the Arctic: Variations, Sources and Trans- port pathways,
724 *J. Geophys. Res.-Atmos.*, 119, 12888–12909, doi:10.1002/2014JD022297, 2014.
- 725 Wang, Q., Jacob, D. J., Fisher, J. A., Mao, J., Leibensperger, E. M., Carouge, C. C., Le Sager, P.,
726 Kondo, Y., Jimenez, J. L., Cubison, M. J., and Doherty, S. J.: Sources of carbonaceous
727 aerosols and deposited black carbon in the Arctic in winter-spring: implications for
728 radiative forcing, *Atmos. Chem. Phys.*, 11, 12453– 12473, doi:10.5194/acp-11-12453-
729 2011, 2011.
- 730 Wang, Q., Jacob, D. J., Spackman, J. R., Perring, A. E., Schwarz, J. P., Moteki, N., Marais, E. A.,
731 Ge, C., Wang, J., and Barrett, S. R. H.: Global budget and radiative forcing of black carbon
732 aerosol: constraints from pole-to-pole (HIPPO) observations across the Pacific, *J.*
733 *Geophys. Res. Atmos.*, 119, 195–206, doi:10.1002/2013JD020824, 2014.
- 734 Winiger, P., Andersson, A., Eckhardt, S., Stohl, A., and Gustafsson, O.: The sources of
735 atmospheric black carbon at a European gateway to the Arctic, *Nat Commun*, 7, 12776,
736 doi:10.1038/ncomms12776, 2016.
- 737 Winiger, P., Barrett, T. E., Sheesley, R. J., Huang, L., Sharma, S., Barrie, L. A., Yttri, K. E.,
738 Evangeliou, N., Eckhardt, S., Stohl, A., Klimont, Z., Heyes, C., Semiletov, I. P., Dudarev, O.
739 V., Charkin, A., Shakhova, N., Holmstrand, H., Andersson, A., and Gustafsson, O.: Source
740 apportionment of circum-Arctic atmospheric black carbon from isotopes and modeling,
741 *Sci Adv*, 5, eaau8052, doi:10.1126/sciadv.aau8052, 2019.
- 742 Xu, J. W., Martin, R. V., Morrow, A., Sharma, S., Huang, L., Leaitch, W. R., Burkart, J., Schulz,
743 H., Zanatta, M., Willis, M. D., Henze, D. K., Lee, C. J., Herber, A. B., and Abbatt, J. P. D.:
744 Source attribution of Arctic black carbon constrained by aircraft and surface
745 measurements, *Atmospheric Chemistry and Physics*, 17, 11971-11989, doi:10.5194/acp-
746 17-11971-2017, 2017.
- 747 [Yang, Y., Wang, H., Smith, S. J., Easter, R. C., and Rasch, P. J.: Sulfate aerosol in the Arctic:
748 Source attribution and radiative forcing, *J. Geophys. Res. Atmos.*, 123, 1899–1918,
749 doi:10.1002/2017JD027298, 2018.](#)
- 750 [Yang, Y., Smith, S. J., Wang, H., Mills, C. M., and Rasch, P. J.: Variability, timescales, and
751 nonlinearity in climate responses to black carbon emissions, *Atmospheric Chemistry and
752 Physics*, 19, 2405–2420, doi:10.5194/acp-19-2405-2019, 2019.](#)
- 753 Yu, K., Keller, C. A., Jacob, D. J., Molod, A. M., Eastham, S. D., and Long, M. S.: Errors and
754 improvements in the use of archived meteorological data for chemical transport

- 755 modeling: an analysis using GEOS-Chem v11-01 driven by GEOS-5 meteorology, *Geosci*
756 *Model Dev*, 11, 305-319, doi:10.5194/gmd-11-305-2018, 2018.
- 757 Zhu, C., Kobayashi, H., Kanaya, Y., and Saito, M.: Size-dependent validation of MODIS
758 MCD64A1 burned area over six vegetation types in boreal Eurasia: Large underestimation
759 in croplands, *Scientific reports*, 7, 4181, doi:10.1038/s41598-017-03739-0, 2017.

Table 1. Comparison of BC source contributions in the Arctic surface

Model and versions	Model type	Wet-deposition	Grid resolution	Meteorology	Emissions	Domain/Sites	Year/season	Major source regions/sectors
Flexpart-WRF 6.2	Lagrangian	Stohl et al. (2005)	unspecified	WRF forecast	ECLIPSE, FINN	continental Norway and Svalbard	spring 2013	Asian anthropogenic
Flexpart 6.2	Lagrangian	Stohl et al. (2005)	1° × 1°	ECMWF operational	Unspecified (BC sensitivities were calculated)	Alert, Barrow, Zeppelin	1989-2009	Northern Eurasia
Flexpart 6.2	Lagrangian	Stohl et al. (2005)	1° × 1°	ECMWF operational	ECLIPSE4(GAINS), GFED3	Arctic (north of 66°N)	2008-2010	Flaring (42%), residential (>20%)
Flexpart 9.2	Lagrangian	Stohl et al. (2005)	1° × 1°	ECMWF operational	ECLIPSE5(GAINS), GFED4.1	Arctic (north of 66.7°N)	2011-2015	Residential and open burning (39%)
Flexpart 10.1	Lagrangian	Grythe et al. (2017)	1° × 1°	ECMWF operational	HTAP2, GFED3, Huang et al. (2015) for Russia flaring	Arctic (north of 66°N)	2010	Flaring (36%), open burning (18%), residential (15%), others (31%)
GEOS-Chem 9.02	CTM	Wang et al. (2011)	2° × 2.5°	GEOS-5	HTAP2, GFED3, Huang et al. (2015) for Russia flaring	Arctic (north of 66°N)	2007-2011	Russia (62%)
GEOS-Chem	CTM	Wang et al. (2011)	2° × 2.5°	GEOS-5	Bond et al. (2004), Zhang et al. (2009), GFED3	Alert, Barrow, Zeppelin	April 2008	Asian anthropogenic (35–45%), Siberian biomass burning (46–64%)
GEOS-Chem	CTM	Wang et al. (2011)	2° × 2.5°	GEOS-5	Bond et al. (2007), FLAMBE	North America Arctic	April 2008	Open fire (50%)

GEOS-Chem10.01	CTM	Wang et al. (2011)	2° × 2.5°	GEOS-5	HTAP2, ECLIPSE5, GFED4	Alert, Barrow, Zeppelin, Arctic (north of 66.5°N)	2009-2011	N-Asian anthropogenic (40–45%) in winter-spring	Xu et al. (2017)
GISS ModelE	GCM	Koch et al. (2006)	4° × 5°	Internal	Bond et al. (2004), Cooke and Wilson (1996)	Arctic (north of ~60°N)	Annual general	South Asia	Koch and Hansen (2005)

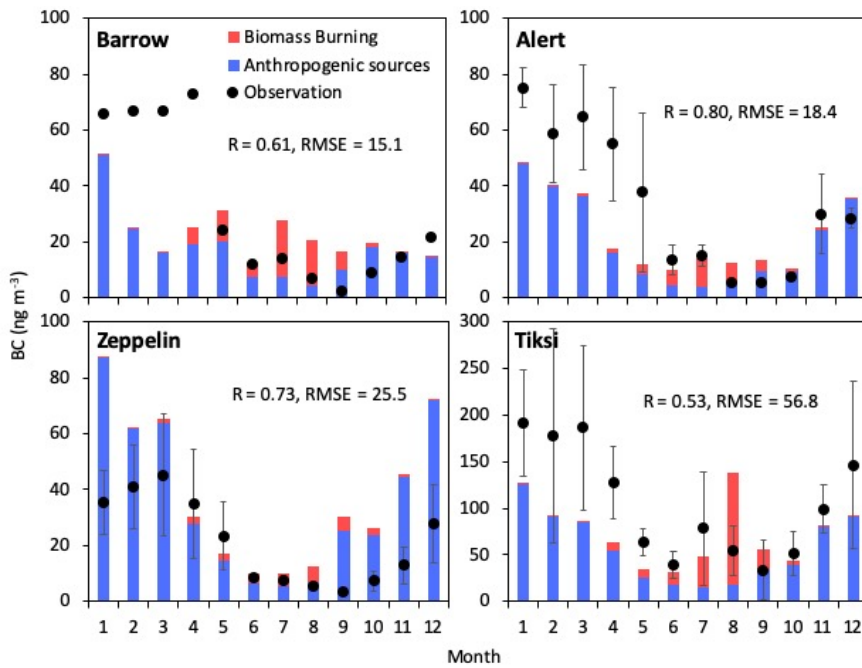


761

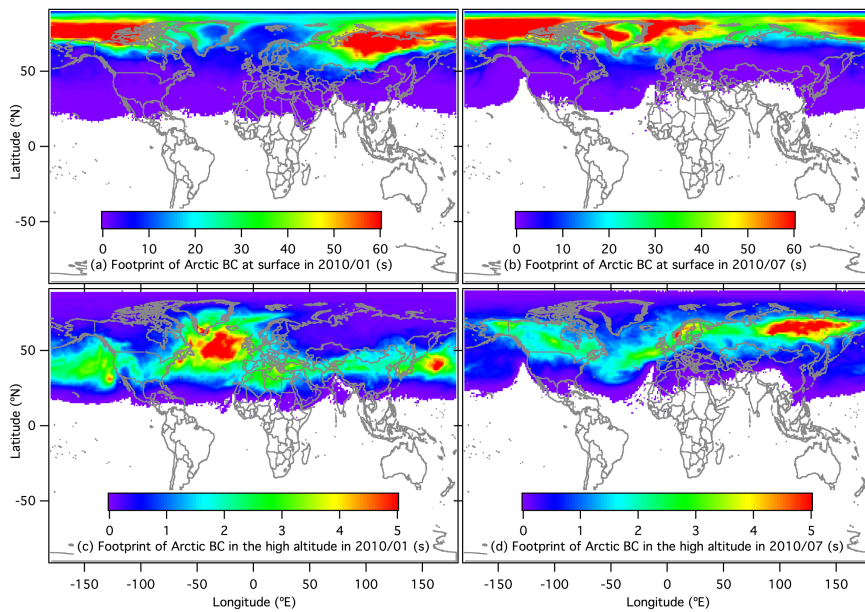
762 Figure 1. Regional separation for quantification of BC in the Arctic from (a) anthropogenic and

763 (b) open biomass burning sources.

764



765
 766 Figure 2. Observed (filled circles) and modeled (bars) seasonal variations in BC mass
 767 concentrations at Arctic sites. Contributions from anthropogenic sources (blue) and open
 768 biomass burning (red) in each month are shown. Monthly averages of observed (filled circles)
 769 and simulated (bars) BC were conducted for 2007–2011 at Alert, Canada (62.3° W , 82.5° N),
 770 and Zeppelin, Norway (11.9° E , 78.9° N), for 2009 at Barrow, USA (156.6° W , 71.3° N), and for
 771 2010–2014 at Tiksi, Russia (128.9° E , 71.6° N). *R* and RMSE indicate correlation coefficient and
 772 root-mean-square error (ng m^{-3}), respectively.
 773

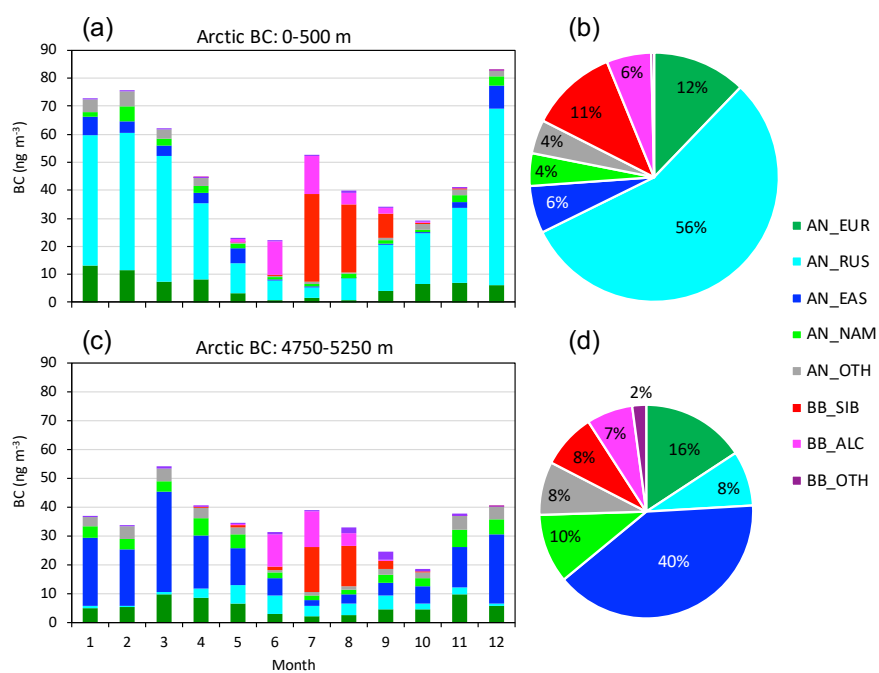


774

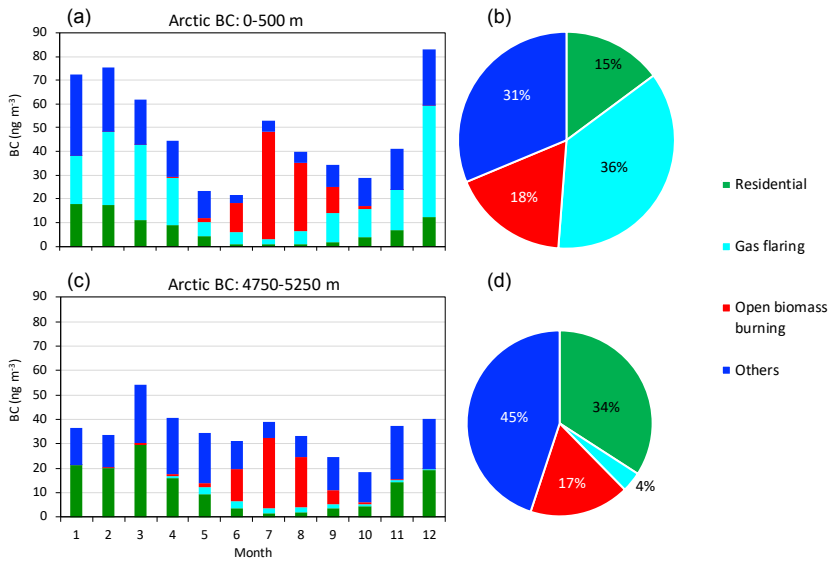
775 Figure 3. Footprints of Arctic BC shown as retention time(s) of (a) BC at surface (0–500 m) in
 776 January 2010, (b) BC at surface in July 2010, (c) BC at high altitudes (4750–5250 m) in January
 777 2010, and (d) BC at high altitudes in July 2010.

778

Deleted: (4750–5250 m)



780
 781 Figure 4. Contributions of anthropogenic sources (prefixed "AN " in the legend) and open
 782 biomass burning ("BB ") from each region to (a) seasonal variations in Arctic surface BC, (b)
 783 annual mean Arctic surface BC, (c) seasonal variations in Arctic BC at high altitudes, and (d)
 784 annual mean of Arctic BC at high altitudes.
 785



786

787 Figure 5. Sectorial contributions from residential combustion (including fossil fuel and biofuel

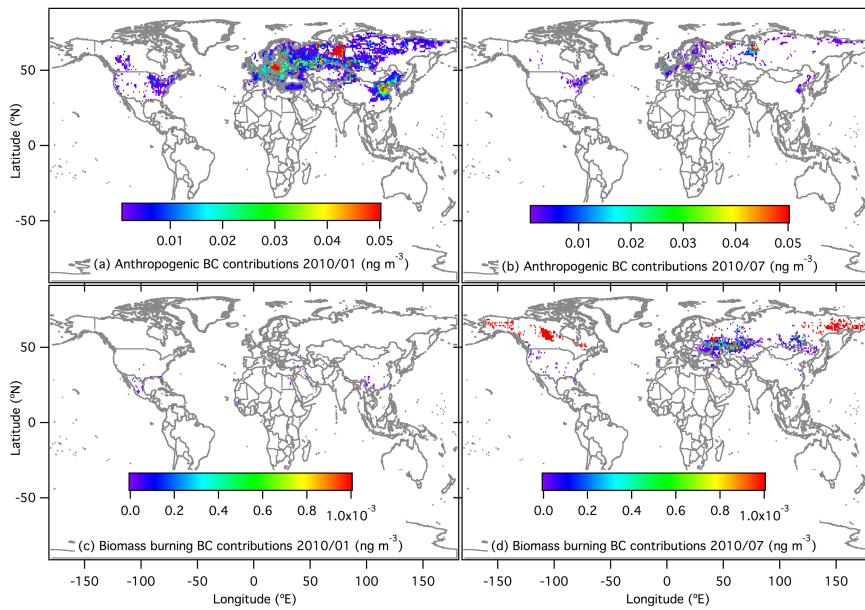
788 combustions), gas flaring, open biomass burning and others (energy other than gas flaring,

789 industry and transport) to (a) seasonal variations in Arctic surface BC, (b) annual mean Arctic

790 surface BC, (c) seasonal variations in Arctic BC at high altitudes, and (d) annual mean of Arctic

791 BC at high altitudes.

792

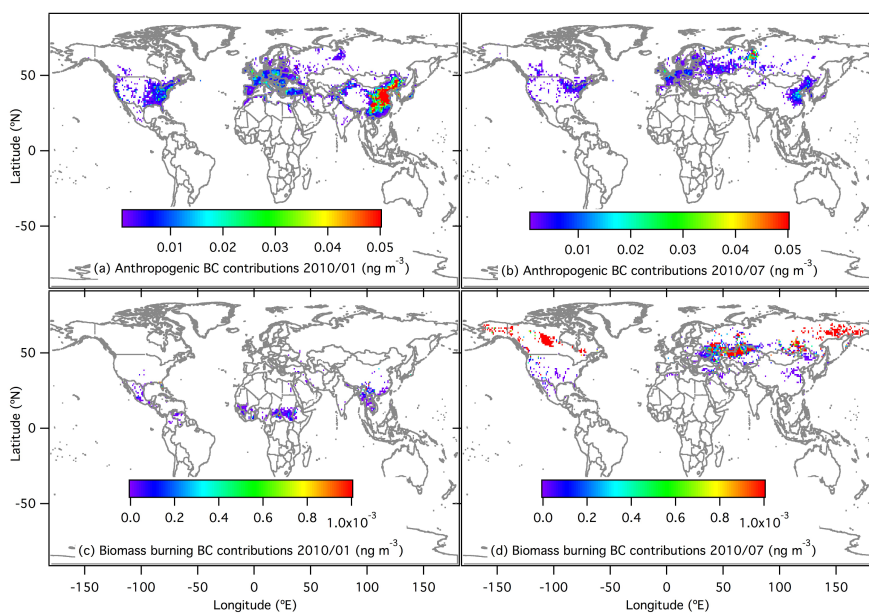


793

794 Figure 6. Spatial distributions of contributions to Arctic BC at surface for (a) anthropogenic
 795 contributions in January 2010, (b) anthropogenic contributions in July 2010, (c) open biomass
 796 burning contributions in January 2010, and (d) open biomass burning contributions in July
 797 2010.

798

Deleted: (0–500 m)



800

801 Figure 7. Spatial distributions of contributions to Arctic BC at high altitudes for (a)
 802 anthropogenic contributions in January 2010, (b) anthropogenic contributions in July 2010, (c)
 803 open biomass burning contributions in January 2010, and (d) open biomass burning
 804 contributions in July 2010.

805

Deleted: (4750–5250 m)